Unique and Overlapping Expression Patterns among Members of Photosynthesis-Associated Nuclear Gene Families in Arabidopsis[1][W][OA]

Megan G. Sawchuk, Tyler J. Donner, Philip Head, and Enrico Scarpella*

Department of Biological Sciences, University of Alberta, Edmonton, Alberta, Canada T6G 2E9

Light provides crucial positional information in plant development, and the morphogenetic processes that are orchestrated by light signals are triggered by changes of gene expression in response to variations in light parameters. Control of expression of members of the *RbcS* and *Lhc* families of photosynthesis-associated nuclear genes by light cues is a paradigm for light-regulated gene transcription, but high-resolution expression profiles for these gene families are lacking. In this study, we have investigated expression patterns of members of the *RbcS* and *Lhc* gene families in Arabidopsis (*Arabidopsis thaliana*) at the cellular level during undisturbed development and upon controlled interference of the light environment. Members of the *RbcS* and *Lhc* gene families are expressed in specialized territories, including root tip, leaf adaxial, abaxial, and epidermal domains, and with distinct chronologies, identifying successive stages of leaf mesophyll ontogeny. Defined spatial and temporal overlap of gene expression fields suggest that the light-harvesting and photosynthetic apparatus may have a different polypeptide composition in different cells and that such composition could change over time even within the same cell.

Plants are exquisitely sensitive to their light environment and have evolved sophisticated biochemical systems to perceive intensity, quality, direction, and duration of the light signal (Chen et al., 2004). Information regarding these parameters is used to modulate an amazing variety of developmental processes throughout the plant's life, thus defining light as one of the most important cues in plant development (Fankhauser and Chory, 1997; Franklin et al., 2005). Most of the events choreographed by light require changes in gene expression (Simpson and Herrera-Estrella, 1990; Thompson and White, 1991), and regulation of gene expression by light, particularly that of the genes encoding the small subunits of the Rubisco (RbcS) and the light-harvesting chlorophyll *a*/*b*-binding proteins (Lhc; previously known as Cab), has been the subject of extensive investigation (Arguello-Astorga and Herrera-Estrella, 1998).

The enzyme Rubisco is located in the stroma of the chloroplast, where it catalyzes the carboxylation of ribulose bisphosphate in the Calvin cycle and the oxygenation of the same substrate in the photorespiratory pathway (Jensen and Bahr, 1977). Rubisco is a multimeric enzyme consisting of eight small subunits and eight large subunits (Baker et al., 1975), and while the large subunits are encoded by a single chloroplast gene (Bedbrook et al., 1979), the small subunits are encoded by a family of nuclear genes (Dean et al., 1989). In Arabidopsis (*Arabidopsis thaliana*), the *RbcS* gene family comprises four members (*RbcS1A*, *RbcS1B*, *RbcS2B*, *RbcS3B*) that have been divided into two subfamilies, A and B, on the basis of linkage and sequence similarities (Krebbers et al., 1988).

Lhc proteins span the chloroplast thylakoid membrane, coordinate the binding of a number of chlorophylls and carotenoids, and, by assembling with the two photosystems, maximize and regulate light harvesting (Grossman et al., 1995). At present, 21 *Lhc* genes have been annotated in Arabidopsis (Jansson, 1994; Klimmek et al., 2006). The *Lhca1* to *Lhca4* genes encode the polypeptides of the light-harvesting complex I (LHCI) associated with the PSI (Jansson, 1994). The LHCI is composed of two heterodimers of Lhca proteins (Lhca1/4 and Lhca2/3) arranged in series (Ben-Shem et al., 2003). Lhca5 monomers or homodimers assemble with the LHCI peripherally at the Lhca2/3 site (Lucinski et al., 2006), while Lhca6 has yet to be characterized. The trimeric LHCII consists of various combinations of three very similar proteins, encoded by the *Lhcb1*, *Lhcb2*, and *Lhcb3* genes (Jansson, 1994). Five *Lhcb1* genes have been characterized (Leutwiler et al., 1986; McGrath et al., 1992), and while the mature proteins encoded by *Lhcb1.1*, *Lhcb1.2*, and *Lhcb1.3* are identical, the Lhcb1.4 and Lhcb1.5 proteins are slightly divergent (Jansson, 1999). Three *Lhcb2* genes have been identified, and the mature proteins

[1] This work was supported by a Discovery Grant of the Natural Sciences and Engineering Research Council of Canada (NSERC), by an Alberta Ingenuity (AI) New Faculty Grant, and by the Canada Research Chairs Program. T.J.D. was supported by an NSERC CGS-M Scholarship and an AI Student Scholarship.

* Corresponding author; e-mail enrico.scarpella@ualberta.ca.

The author responsible for distribution of materials integral to the findings presented in this article in accordance with the policy described in the Instructions for Authors (www.plantphysiol.org) is: Enrico Scarpella (enrico.scarpella@ualberta.ca).

[W] The online version of this article contains Web-only data.

[OA] Open Access articles can be viewed online without a subscription.

www.plantphysiol.org/cgi/doi/10.1104/pp.108.126946

encoded by *Lhcb2.1* and *Lhcb2.2* are identical, while Lhcb2.3 differs by only one amino acid (Jansson, 1999; Klimmek et al., 2006). Lhcb3 is encoded by a single gene (Jansson, 1999). The Lhcb4, Lhcb5, and Lhcb6 proteins are associated with the PSII in monomeric aggregation states (Jansson, 1994), while Lhcb7 and Lhcb8 have not yet been characterized. The two *Lhcb4* genes, *Lhcb4.1* and *Lhcb4.2*, encode proteins that display a low level of sequence identity (Jansson, 1999). Single genes encode Lhcb5, Lhcb6, Lhcb7, and Lhcb8 (Jansson, 1999; Klimmek et al., 2006).

The influence of light on regulation of *RbcS* and *Lhc* expression is exerted at multiple levels (Tobin and Silverthorne, 1985; Simpson and Herrera-Estrella, 1990; Thompson and White, 1991; Terzaghi and Cashmore, 1995). Light affects transcription of *RbcS* and *Lhc* genes, as well as the stability and translation of their transcripts. Furthermore, light has been implicated in the regulation of a variety of posttranslational processes controlling RbcS and Lhc activity, including protein folding, localization, and assembly of polypeptides into protein complexes. Because RbcS and Lhc proteins can interact within each family to form heterodimers, trimers, and higher-order complexes, the activity of the resulting entities could vary depending on their composition, should the different subunits have different biochemical properties. The composition of RbcS and Lhc protein complexes would ultimately depend on which subsets of compatible partners were simultaneously expressed in the same cells and could change under different regimes, were the single constituents differentially regulated by environmental signals. In a wide array of species, individual members of the *RbcS* and *Lhc* families have been shown to display a range of expression levels in different organs, with stereotypically strong expression in leaves, significantly lower expression in other green organs, and very low, if any, expression in organs devoid of chloroplasts (Tobin and Silverthorne, 1985; Dean et al., 1989; Simpson and Herrera-Estrella, 1990; Thompson and White, 1991). However, high-resolution expression profiles in the homologous system are available only for selected members of the *RbcS* and *Lhc* families, specific organs, and few species (e.g. Jefferson et al., 1987; Langdale et al., 1988; Silverthorne and Tobin, 1990; Bansal et al., 1992; Meier et al., 1995; Fleming et al., 1996), and are lacking for any of the *RbcS* and *Lhc* genes in Arabidopsis.

Here, we have characterized expression patterns of Arabidopsis *RbcS* and *Lhc* genes at cellular resolution during undisturbed development and upon controlled light context interference. Our data show that despite the large degree of overlap among gene expression patterns, individual members of the *RbcS* and *Lhc* families are associated with unique spatio-temporal expression profiles. Furthermore, our results suggest that expression of defined sets of *RbcS* and *Lhc* genes identifies distinct stages of leaf tissue ontogeny that cannot be distinguished anatomically. By charting a geography of the possible RbcS and Lhc protein complexes in different cells and tissues under normal and challenged development, we finally supply a platform for future functional studies aimed at dissecting the specialized and redundant roles of the members of these gene families.

RESULTS

Visualization of *RbcS* and *Lhc* Expression

Because regulation of *RbcS* and *Lhc* expression is accomplished, at least in part, at the transcriptional level (Tobin and Silverthorne, 1985; Simpson and Herrera-Estrella, 1990; Thompson and White, 1991; Terzaghi and Cashmore, 1995), we employed transcriptional reporter gene fusions to visualize *RbcS* and *Lhc* expression patterns at high resolution.

While analysis of global gene expression data for the *RbcS* family is not available, expression profiling has recently shown that the abundantly expressed *Lhca1* to *Lhca4* and *Lhcb1* to *Lhcb6* are coregulated in Arabidopsis, although within that cluster, *Lhcb6*, *Lhcb4.1*, *Lhcb4.2*, and *Lhcb2.3* are expressed with a partially divergent pattern (Klimmek et al., 2006). Furthermore, the four rarely expressed *Lhca5*, *Lhca6*, *Lhcb7*, and *Lhcb8* have been shown to display a distinct regulation profile from that of the abundantly expressed *Lhc* genes (Klimmek et al., 2006). Therefore, we have here sampled all the *RbcS* genes, seven representative members of the abundantly expressed *Lhc* genes, including three of the four genes displaying slightly deviant expression, and three of the four rarely expressed *Lhc* genes (Supplemental Table S1).

The sequence within 3 kb upstream of the translation start codon is sufficient to recapitulate the endogenous mRNA expression pattern in 80% of the cases for 44 Arabidopsis transcription factors (Lee et al., 2006). Therefore, to construct transcriptional fusions of *RbcS* and *Lhc* genes, we used approximately 3 kb of upstream noncoding sequence, whenever primer design made it possible, or the entire upstream noncoding region, whichever was shorter (Supplemental Table S1).

To improve the sensitivity and spatial resolution for detecting gene expression, all the upstream regulatory sequences generated in our study were fused to a nuclear-localized yellow fluorescent protein (YFP) that consists of a translational fusion between the coding region of histone 2A (HTA6; At5g59870) and that of the enhanced YFP (EYFP; Zhang et al., 2005). Because YFP is approximately 50% brighter than GFP and four times brighter than the cyan fluorescent protein (CFP; Dobbie et al., 2008), we reasoned that YFP should allow us to detect fusions at much lower expression levels. Furthermore, because YFP signals can be easily separated from both CFP and GFP fluorescence in plants (e.g. Kato et al., 2002; Sawchuk et al., 2007), YFP fusions should greatly expand the number of possible combinations with preexisting fluorescent marker

lines and consequently vastly increase the utility of the resources generated here. Targeting all the YFP produced in each individual cell to the nucleus locally increases the concentration of YFP of 30% to 50%, resulting in enhanced sensitivity of signal detection (Joly, 2007). Furthermore, nuclear localization of YFP allows sufficient spatial separation from coexpressed plasma membrane-targeted fluorescent labels necessary to determine the shape of YFP-expressing cells (see below).

The expression profile conferred by the *RbcS* and *Lhc* regulatory sequences was characterized in transgenic Arabidopsis. For each construct, the progeny of 10 to 18 independent transgenic lines were inspected to identify the most representative expression pattern. Detailed expression analysis was performed on the progeny of three homozygous lines per construct. These representative lines were selected based on strong YFP expression, emblematic of the expression profile observed across the entire series of transgenic lines and resulting from single insertion of the transgene. In genetic crosses, the progeny of at least two independent transgenic lines per construct were examined. Attributes used to assess the representative nature of the displayed features and derived reproducibility quotients are reported in Supplemental Table S2. Higher-resolution images are provided in Supplemental Figures S1 to S7.

RbcS and *Lhc* Expression in Light-Grown Seedlings

We first asked whether *RbcS* and *Lhc* genes were expressed in specific cellular domains within organs of light-grown seedlings. To address this question, we imaged $RbcS_{pro}$:HTA6:EYFP and Lhc_{pro}:HTA6:EYFP expression in whole seedlings and in cotyledons, hypocotyl, and root of seedlings 4 d after germination (DAG). Detected fluorescence signals were digitized with analog-to-digital converters that support 4096 discrimination levels, and individual images were acquired using the full extent of such resolution (see "Materials and Methods"); however, our eyes can only distinguish few tens of shades of gray (Russ, 2002). Therefore, to fully and readily convey information on fluorescence feature properties, monochrome images were color displayed with a purposely created look-up table (LUT; available as downloadable supplementary file) in which black was used to encode global background, blue to encode local background, and cyan, green, yellow, orange, and red to encode increasing signal intensities (Fig. 1, A–C).

All *RbcS* and *Lhc* genes were expressed in cotyledons (Figs. 1, A and C–P, and 2, A, D, G, J, M, P, S, V, Y, AB, AE, AH, AK, and AN). However, while expression of a few genes was uniformly distributed (*RbcS1B* and *RbcS3B*) or randomly scattered (*Lhcb2.1*, *Lhcb2.3*, *Lhcb4.1*, and *Lhcb8*) throughout the entire cotyledon (Fig. 2, D, J, V, Y, AB, and AN), most of the genes showed preferential or exclusive expression to the basal region of the cotyledon (Fig. 2, A, G, M, P, S, AE,

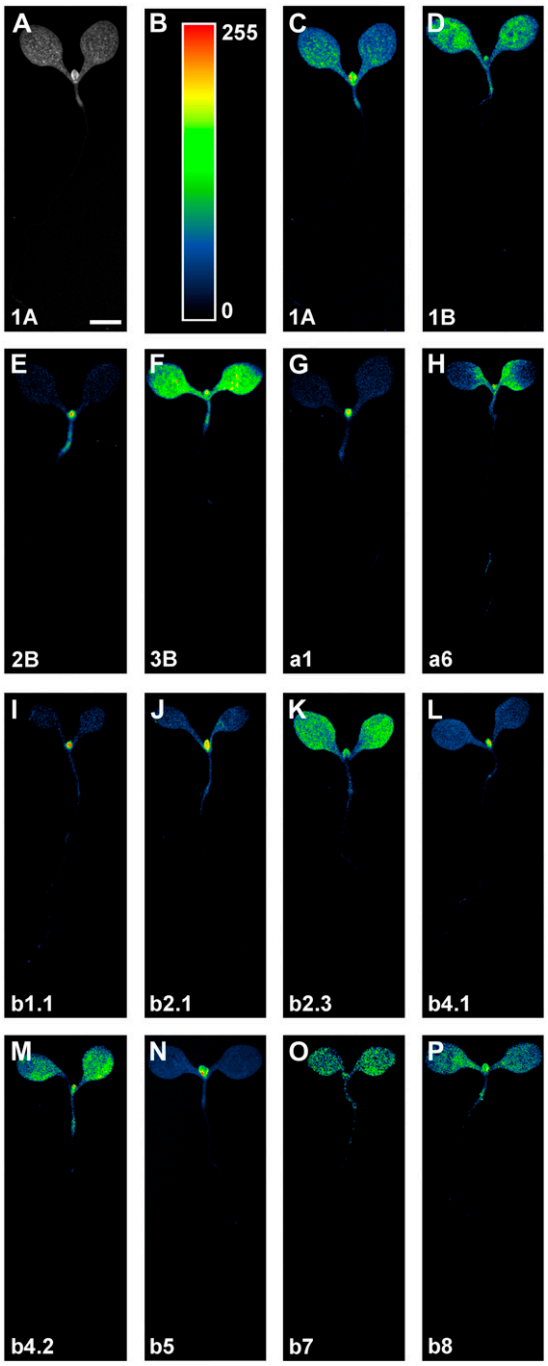

Figure 1. *RbcS* and *Lhc* expression in light-grown seedlings. Bottom left, Gene identity. Seedlings are displayed at identical magnification; therefore, for simplicity, a scale bar is only reported in the first image. A and C to P, Wide-field epifluorescence microscopy. A to C, A LUT in which black was used to encode global background, blue to encode local background, and cyan, green, yellow, orange, and red to encode increasing signal intensities (B) was applied to eight-bit gray-scaled images (A) to generate color-coded images (C). For additional details, see text. 1A, *RbcS1A*; 1B, *RbcS1B*; 2B, *RbcS2B*; 3B, *RbcS3B*; a1, *Lhca1*; a6, *Lhca6*; b1.1, *Lhcb1.1*; b2.1, *Lhcb2.1*; b2.3, *Lhcb2.3*; b4.1, *Lhcb4.1*; b4.2, *Lhcb4.2*; b5, *Lhcb5*; b7, *Lhcb7*; b8, *Lhcb8*. Bar: 500 μm.

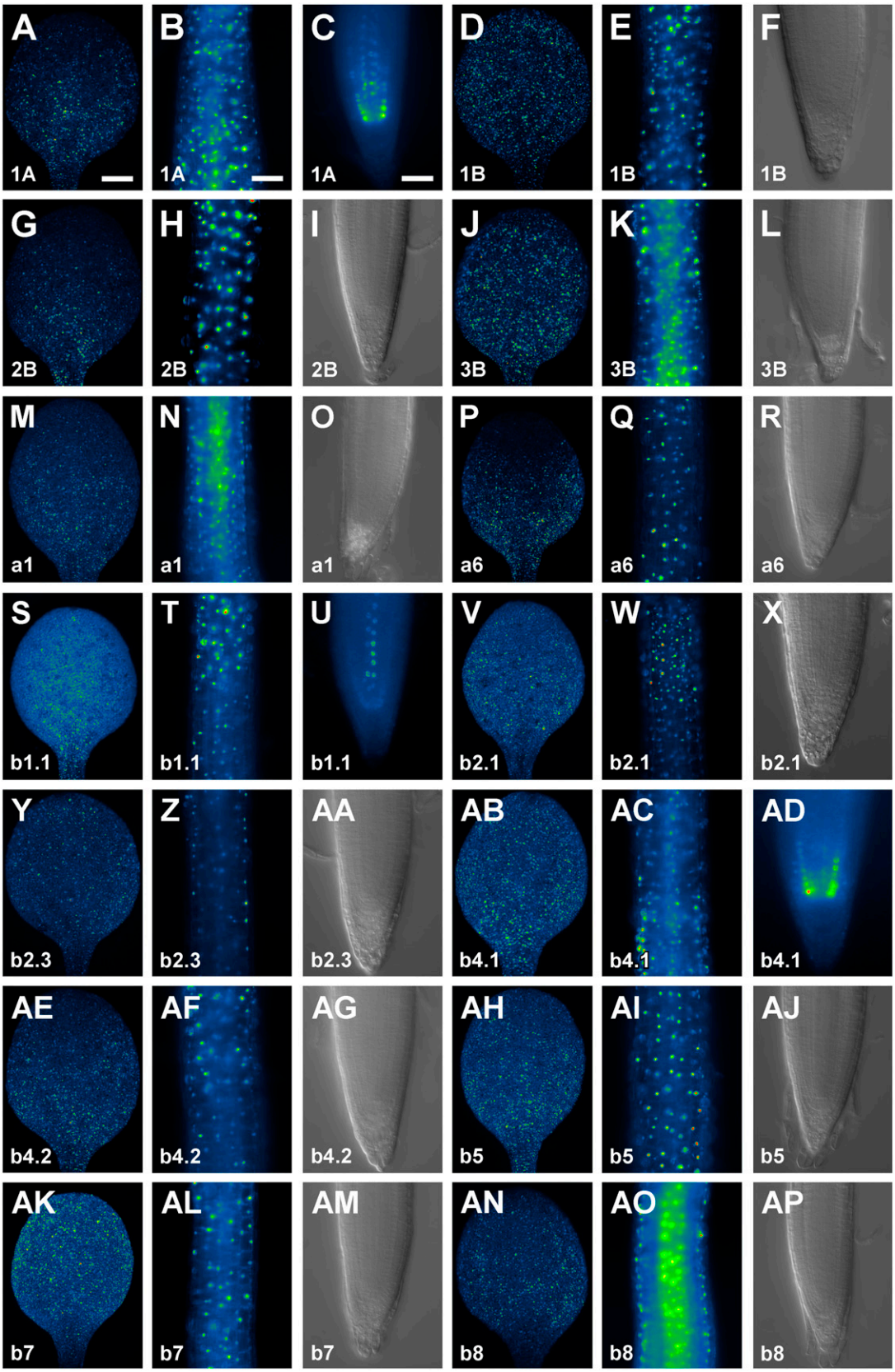

Figure 2. *RbcS* and *Lhc* expression in seedling organs. In-figure information, color code, and abbreviations are as described in Figure 1. Equivalent organs are displayed at identical magnification; therefore, for simplicity, scale bars are only reported in the

and AH), and only *Lhcb7* expression was slightly more pronounced in the apical portion of the cotyledon (Fig. 2AK). In general, *RbcS* and *Lhc* genes were evenly expressed along the hypocotyl (Figs. 1, A and C–P, and 2, B, E, H, K, N, Q, T, W, Z, AC, AF, AI, AL, and AO). Finally, expression of *RbcS* and *Lhc* genes was prevalently absent in roots (Fig. 2, F, I, L, O, R, X, AA, AG, AJ, AM, and AP), but *Lhcb1.1* was expressed in vascular cells (Fig. 2U), *Lhcb4.1* in the endodermis (Fig. 2AD), and *RbcS1A* in both vascular and endodermal cells (Fig. 2C).

RbcS and *Lhc* Expression in Mature Plant Organs and Embryos

We next asked whether *RbcS* and *Lhc* genes were expressed in distinctive cellular territories of mature plant organs and embryos. To address this question, we visualized $RbcS_{pro}$:HTA6:EYFP and Lhc_{pro}:HTA6:EYFP expression in first leaves of seedlings 14 DAG, in flowers at stages 13 to 15 (Smyth et al., 1990) of plants at the onset of stage 1, at which the first silique has differentiated on the inflorescence (approximately 25 DAG; Altamura et al., 2001), and in stems, siliques, and embryos of plants at the end of stage 2, at which all flowers have differentiated into green siliques (approximately 40 DAG; Altamura et al., 2001).

In mature first leaves, most *RbcS* and *Lhc* genes were expressed profusely and without a marked bias (Fig. 3, A, F, P, U, AE, AJ, AO, AY, BD, and BN), except for *RbcS2B*, which showed predominant expression toward the basal portion of the leaf (Fig. 3K). Only *Lhca6*, *Lhcb4.1*, and *Lhcb7* showed erratic, inconspicuous expression in mature first leaves (Fig. 3, Z, AT, and BI). With the exception of *Lhcb4.1*, all *RbcS* and *Lhc* genes were expressed in the mature, lowermost region of the stem (Fig. 3, B, G, L, Q, V, AA, AF, AK, AP, AU, AZ, BE, BJ, and BO). Most of the genes were expressed there ubiquitously (Fig. 3, B, G, Q, V, AF, AK, AP, AZ, BE, and BO), but expression of *RbcS2B*, *Lhca6*, and *Lhcb7* was restricted to the cortex (Fig. 3, L, AA, and BJ). All *RbcS* and *Lhc* genes, with the exception of *Lhcb4.2*, were expressed in mature flowers (Fig. 3, C, H, M, R, W, AB, AG, AL, AQ, AV, BA, BF, BK, and BP). Most of the genes were expressed in both sepals and petals (Fig. 3, C, H, M, R, W, AG, AL, AQ, BF, BK, and BP), while *Lhca6* was expressed in the sepals only (Fig. 3AB) and *Lhcb4.1* was exclusively expressed in petals (Fig. 3AV). Except for *Lhcb4.1*, all *RbcS* and *Lhc* genes were expressed in mature green siliques (Fig. 3, D, I, N, S, X, AC, AH, AM, AR, AW, BB, BG, BL, and BQ). Finally, expression of *RbcS* and *Lhc* genes was typically absent in mature embryos (Fig. 3, J, O, T, Y, AI, AS, AX, BC, and BH), but was detected in the root tip for *RbcS1A* and *Lhcb8* (Fig. 3, E and BR) and in the cotyledons and embryonic axis for *Lhca6*, *Lhcb2.1*, and *Lhcb7* (Fig. 3, AD, AN, and BM).

RbcS and *Lhc* Expression during Leaf Development

All *RbcS* and *Lhc* genes are expressed in mature foliar organs (Figs. 1–3); however, their patterns of initiation, progression, and termination, or persistence, of expression could be remarkably different, even for genes that are expressed similarly at organ maturity. To visualize dynamics of *RbcS* and *Lhc* expression over time, we monitored $RbcS_{pro}$:HTA6:EYFP and Lhc_{pro}:HTA6:EYFP expression in first leaves at 2.5, 4, and 6 DAG.

At 2.5 DAG, most of the *RbcS* and *Lhc* genes were expressed throughout the primordia with the exception of its middle region (Fig. 4, A, G, J, M, P, S, V, AB, AE, and AH). At 4 DAG, expression of a subset of those genes (*RbcS2B*, *Lhca6*, *Lhcb2.1*, *Lhcb4.1*, and *Lhcb5*) comprised the most apical half of the leaves (Fig. 4, H, Q, W, AC, and AI) and pervaded the entire leaves at 6 DAG (Fig. 4, I, R, X, AD, and AJ). Expression of the complementary subset of genes (*RbcS1A*, *RbcS3B*, *Lhca1*, *Lhcb1.1*, and *Lhcb4.2*) was restricted to the most apical one-third of the 4-DAG leaves (Fig. 4, B, K, N, T, and AF), and by 6 DAG, expression encompassed the apical two-thirds of the leaves (Fig. 4, C, L, O, U, and AG). While most of the *RbcS* and *Lhc* genes were therefore expressed in largely overlapping spatial domains and with strikingly comparable temporal dynamics, a few *RbcS* and *Lhc* genes were expressed with conspicuously distinct patterns. *Lhcb2.3* expression was absent in 2.5-DAG primordia, was constrained to the leaf tip at 4 DAG, and embraced the most apical one-half of 6-DAG leaves (Fig. 4, Y–AA). *RbcS1B* was expressed with an unequivocal preference for the abaxial side of 2.5-DAG primordia, and expression remained confined to the abaxial side of 4- and 6-DAG leaves (Fig. 4, D–F; Supplemental Fig. S8). In contrast, *Lhcb7* showed pronounced adaxial expression throughout leaf development, and expression at the abaxial side was largely circumscribed to the leaf tip (Fig. 4, AK–AM). Finally, *Lhcb8* was expressed with a prominent epidermal bias at all stages of leaf development (Fig. 4, AN–AP).

We next asked whether inception of *RbcS* and *Lhc* expression could be assigned to specific stages of leaf subepidermal cell development. We selected expression of *RbcS2B*, *RbcS3B*, and *Lhcb2.3* as representatives of three different chronologies of gene expression (Fig. 4, A–AP), and adopted the combination of cell mor-

Figure 2. (*Continued.*)
first image of the respective organ series. A to E, G, H, J, K, M, N, P, Q, S to W, Y, Z, AB to AF, AH, AI, AK, AL, AN, and AO, Wide-field epifluorescence microscopy. F, I, L, O, R, X, AA, AG, AJ, AM, and AP, Differential interference contrast microscopy. A, D, G, J, M, P, S, V, Y, AB, AE, AH, AK, and AN, Cotyledons, adaxial view. B, E, H, K, N, Q, T, W, Z, AC, AF, AI, AL, and AO, Hypocotyls. C, F, I, L, O, R, U, X, AA, AD, AG, AJ, AM, and AP, Root tips. Bars: A, 150 μm; B, 150 μm; C, 50 μm.

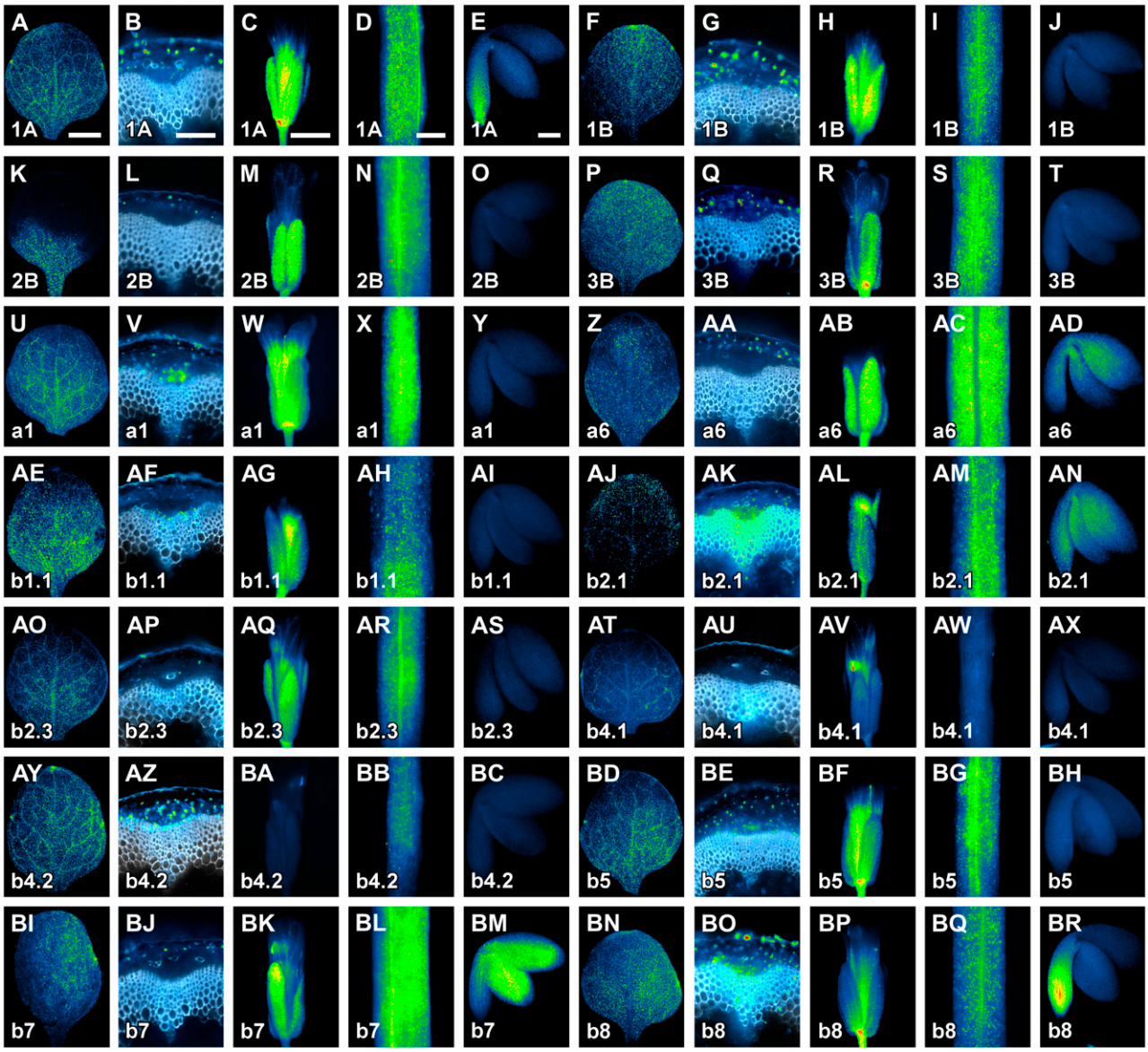

Figure 3. *RbcS* and *Lhc* expression in mature plant organs and embryos. In-figure information, color code, and abbreviations are as described in Figure 1. Equivalent organs are displayed at identical magnification; therefore, for simplicity, scale bars are only reported in the first image of the respective organ series. Wide-field epifluorescence microscopy throughout. A, F, K, P, U, Z, AE, AJ, AO, AT, AY, BD, BI, and BN, First leaves 14 DAG, abaxial view. B, G, L, Q, V, Z, AA, AF, AK, AP, AU, AZ, BE, BJ, and BO, Cross sections through the lowermost region of the stem of plants at stage 2 (Altamura et al., 2001); white, lignin autofluorescence. C, H, M, R, W, AB, AG, AL, AQ, AV, BA, BF, BK, and BP, Flowers at stages 13 to 15 (Smyth et al., 1990). D, I, N, S, X, AC, AH, AM, AR, AW, BB, BG, BL, and BQ, Mature siliques of plants at stage 2. E, J, O, T, Y, AD, AI, AN, AS, AX, BC, BH, BM, and BR, Mature embryos of plants at stage 2. Bars: A and D, 1 mm; B and E, 100 μm; C, 250 μm.

phology, extent of intercellular spaces, and level of plastid intrinsic fluorescence as a stage-specific indicator of leaf subepidermal cell differentiation (Pyke and Page, 1998; Scarpella et al., 2004; Kang et al., 2007). We visualized onset of RbcS2B$_{pro}$:HTA6:EYFP, RbcS3B$_{pro}$:HTA6:EYFP, and Lhcb2.3$_{pro}$:HTA6:EYFP expression in 4-DAG leaves of the plasma membrane marker line UBQ10$_{pro}$:EGFP:LTi6b. *RbcS2B* and *RbcS3B* were first expressed in tightly connected polygonal cells (Fig. 4, AQ, AR, AT, and AU); however, unlike *RbcS2B*, onset of *RbcS3B* expression was associated with presence of weakly autofluorescent plastids (Fig. 4, AS–AU). Finally, initiation of *Lhcb2.3* expression occurred in expanded cells that had acquired a distinctively round shape, that contained large numbers of strongly autofluorescent plastids along the cell surface, and that were separated by conspicuous intercellular spaces (Fig. 4AV).

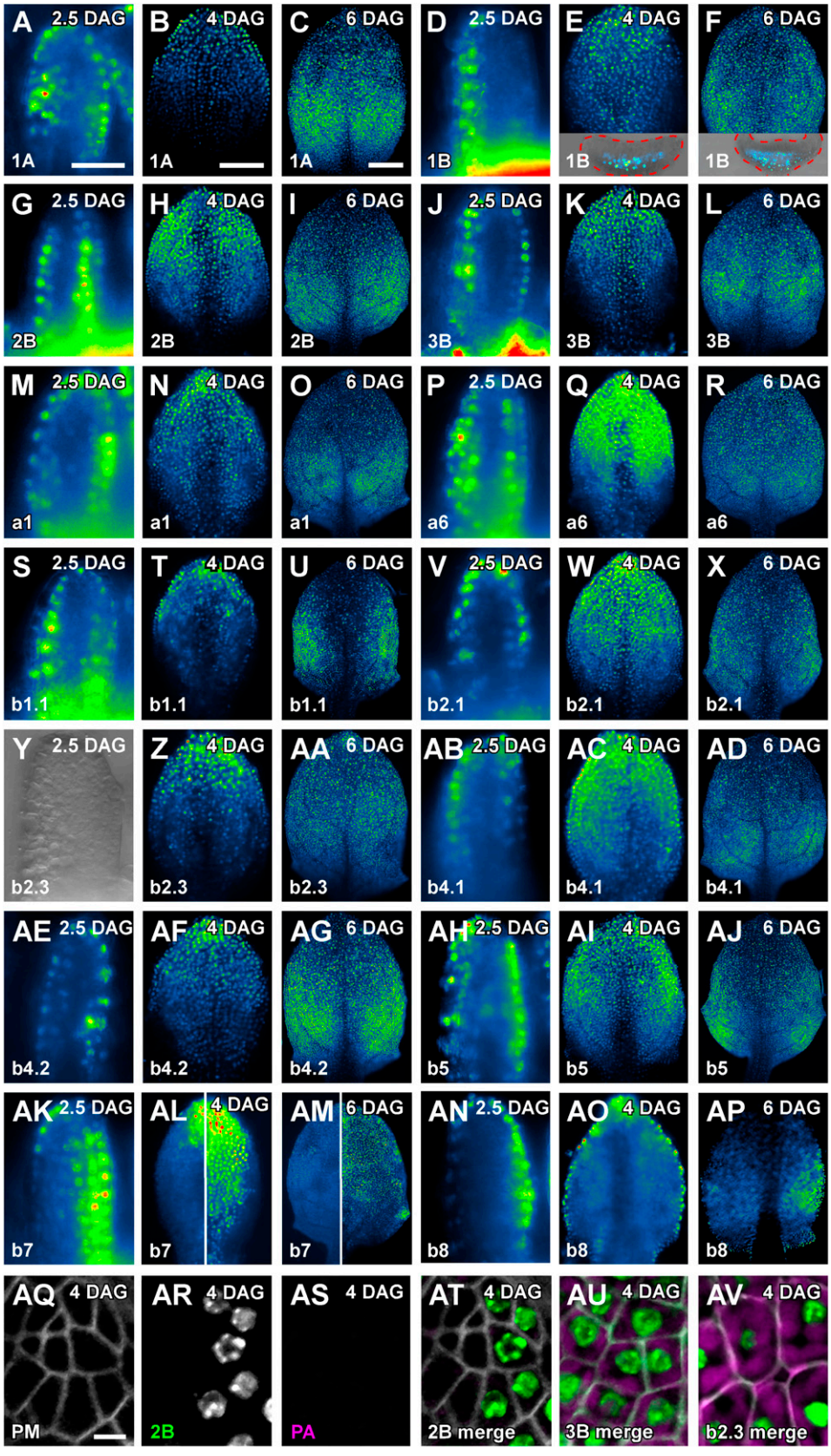

Figure 4. *RbcS* and *Lhc* expression during leaf development. In-figure information, color code, and abbreviations are as described in Figure 1. Top right: leaf primordium age in DAG. Leaf primordia at equivalent DAG are displayed at identical magnification; therefore, for simplicity, scale bars are only reported in the first image of the respective DAG series. A to X and Z to AP, Wide-field epifluorescence microscopy. Y, Differential interference contrast microscopy. AQ to AV, Confocal laser scanning microscopy. A, D, G, J, M, P, S, V, Y, AB, AE, AH, AK, and AN, Lateral view (adaxial side of primordia to the right). B, C, E, F, H, I, K, L, N, O, Q, R, T, U, W, X, Z, AA, AC, AD, AF, AG, AI, AJ, AL (left side), AM (left side), and AO to AV, Abaxial view. AL (right side) and AM (right side), Adaxial view. Insets in E and F, Overlay between wide-field epifluorescent and differential interference contrast microscopy images of cross sections through the middle of 4- and 6-DAG leaves, respectively; red dashed line, primordium outline; adaxial side toward top. AQ, Plasma membrane-labeling $UBQ10_{pro}$:EGFP:LTi6b expression. AR, $RbcS2B_{pro}$:HTA6:EYFP expression. AS, Plastid autofluorescence. AT, Overlay of images in AQ-AS; note that cells expressing $RbcS2B_{pro}$:HTA6:EYFP cannot be anatomically discriminated from neighboring cells. AU, Overlay of images of $UBQ10_{pro}$:EGFP:LTi6b and $RbcS3B_{pro}$:HTA6:EYFP expression and of plastid autofluorescence. AV, Overlay of images of $UBQ10_{pro}$:EGFP:LTi6b and $Lhcb2.3_{pro}$:HTA6:EYFP expression and of plastid autofluorescence. Images of plastid autofluorescence were all acquired at identical settings (see "Materials and Methods" for details). PA, Plastid autofluorescence; PM, Plasma membrane. Bars: A and B, 50 μm; C, 200 μm; AQ, 5 μm.

Cell and Tissue-Specific Expression of *RbcS* and *Lhc* Genes in Foliar Organs

Despite their different dynamics during leaf development, *RbcS* and *Lhc* expression seemed to be excluded from leaf veins (Fig. 4). An unambiguous criterion to test such a hypothesis would be to visualize expression of *RbcS* and *Lhc* genes relative to that of the early vascular marker gene *Athb8* (Baima et al., 1995). Onset of *Athb8* gene expression in leaves labels a subset of ground cells that have been specified to vascular cell fate (i.e. preprocambial cells) but that are morphologically indistinguishable from the residual ground cell population (Kang and Dengler, 2004; Scarpella et al., 2004). We therefore rigorously assessed the degree of colocalization between $RbcS_{pro}$:HTA6:EYFP and Lhc_{pro}:HTA6:EYFP on the one hand and $Athb8_{pro}$:ECFP:3xNLS on the other. Because of the differential sensitivity of our perception across the visible spectrum (Russ, 2002), to improve discrimination of fluorescence signals in double-labeling images and therefore more accurately visualize signal colocalization, we adopted an extended dual-channel LUT from cyan to magenta through green, yellow, and red (Demandolx and Davoust, 1997). Fluorescence in each detection channel was displayed in either cyan (e.g. Fig. 5A) or magenta (e.g. Fig. 5B). Single-fluorophore images were then merged using a differential operator (see "Materials and Methods"). As a result, preponderance of cyan signal over colocalized magenta signal is encoded in green, opposite in red, and colocalized cyan and magenta signals of equal intensity in yellow (e.g. Fig. 5C). As shown in Figure 5, none of the *RbcS* and *Lhc* genes was expressed in *Athb8*-labeled cells, suggesting that *RbcS* and *Lhc* gene expression is excluded from vascular cells, already at the preprocambial stage. To test for possible artifacts induced by fluorophore intrinsic properties (e.g. different maturation time and stability of HTA6:EYFP and ECFP:3xNLS) or detection parameters (e.g. suboptimal excitation wavelength and emission interval), we exchanged fluorophores for the *RbcS2B* and *Athb8* gene expression combination and measured extent of colocalization between $RbcS2B_{pro}$:ECFP:3xNLS and $Athb8_{pro}$:HTA6:EYFP signals (Fig. 5R). The absence of any overlap of fluorescence in reciprocal permutations of *RbcS2B* and *Athb8* regulatory regions with YFP and CFP (compare Fig. 5, F and R) suggests that our colocalization data are fluorophore independent, thus further supporting that *RbcS* and *Lhc* genes are not expressed in leaf preprocambial cells.

While *Lhcb8* was exclusively expressed in epidermal cells of the leaf (Figs. 4, AN–AP, and 5Q), we asked whether expression of *RbcS* genes and of all other *Lhc* genes was confined to subepidermal, nonvascular cells. To address this question, we visualized $RbcS_{pro}$:HTA6:EYFP and Lhc_{pro}:HTA6:EYFP expression in epidermis of 4-DAG cotyledons in which plasma membranes were labeled by the FM 4-64 water-soluble lipophilic dye to expose cell shape. As shown in Figure 6, all genes, with the sole exception of *Lhca6* and *Lhcb1.1*, were expressed in guard cells of stomata.

Response of *RbcS* and *Lhc* Expression to Different Light Conditions

Levels of *RbcS* and *Lhc* expression are strongly affected by light signals (Tobin and Silverthorne, 1985; Simpson and Herrera-Estrella, 1990; Thompson and White, 1991; Terzaghi and Cashmore, 1995; Arguello-Astorga and Herrera-Estrella, 1998). We therefore finally asked whether light cues also impinged on the spatial patterns of *RbcS* and *Lhc* expression. To address this question, we grew seedlings for 3 d in the dark and either transferred them to blue, red, or far-red light conditions (see "Materials and Methods") or continued to grow them in the dark. We then visualized $RbcS_{pro}$:HTA6:EYFP and Lhc_{pro}:HTA6:EYFP expression at 4 DAG.

While elevation of *Lhcb7* expression was selectively elicited by blue and far-red light treatments, enhanced expression of all other *RbcS* and *Lhc* genes was induced by light, although at different levels, irrespective of its spectrum range (Fig. 7). However, responsiveness of gene expression to light was constrained by organ-specific cues. In fact, while induction of expression for most genes was restricted to cotyledons (Fig. 7, E–L, Q–T, Y–AB, AG–AN, and AW–AZ), a few genes (*RbcS1A*, *Lhcb2.1*, and *Lhcb4.2*) displayed light-stimulated enhancement of expression in both cotyledons and hypocotyls (Fig. 7, A–D, AC–AF, and AO–AR). Furthermore, expression of *RbcS3B*, *Lhca6*, *Lhcb5*, and *Lhcb8* was induced in both cotyledons and hypocotyls in blue and far-red light but solely in the cotyledons in red light (Fig. 7, M–P, U–X, AS–AV, and BA–BD). Finally, up-regulation of *RbcS* and *Lhc* gene expression was not observed in the root (not shown).

DISCUSSION

Global gene expression profiling provides invaluable information on gene expression levels and their regulation at whole-genome scale, but is typically characterized by a limited degree of discrimination in the spatial dimension (Kehr, 2003; Brandt, 2005; Lange, 2005; Lee et al., 2005). High-resolution gene expression analysis is therefore the perfect complement to ongoing genome-wide approaches to the study of transcript accumulation patterns. In this study, we have investigated expression patterns of members of the *RbcS* and *Lhc* photosynthesis-associated nuclear gene families in Arabidopsis at the cellular level during undisturbed development and upon controlled light context interference. Transcription of *RbcS* and *Lhc* genes could be modulated by regions other than the upstream regulatory sequences used in our study (e.g. Ali and Taylor, 2001). Furthermore, abundance of *RbcS* and *Lhc* transcripts can be regulated at the

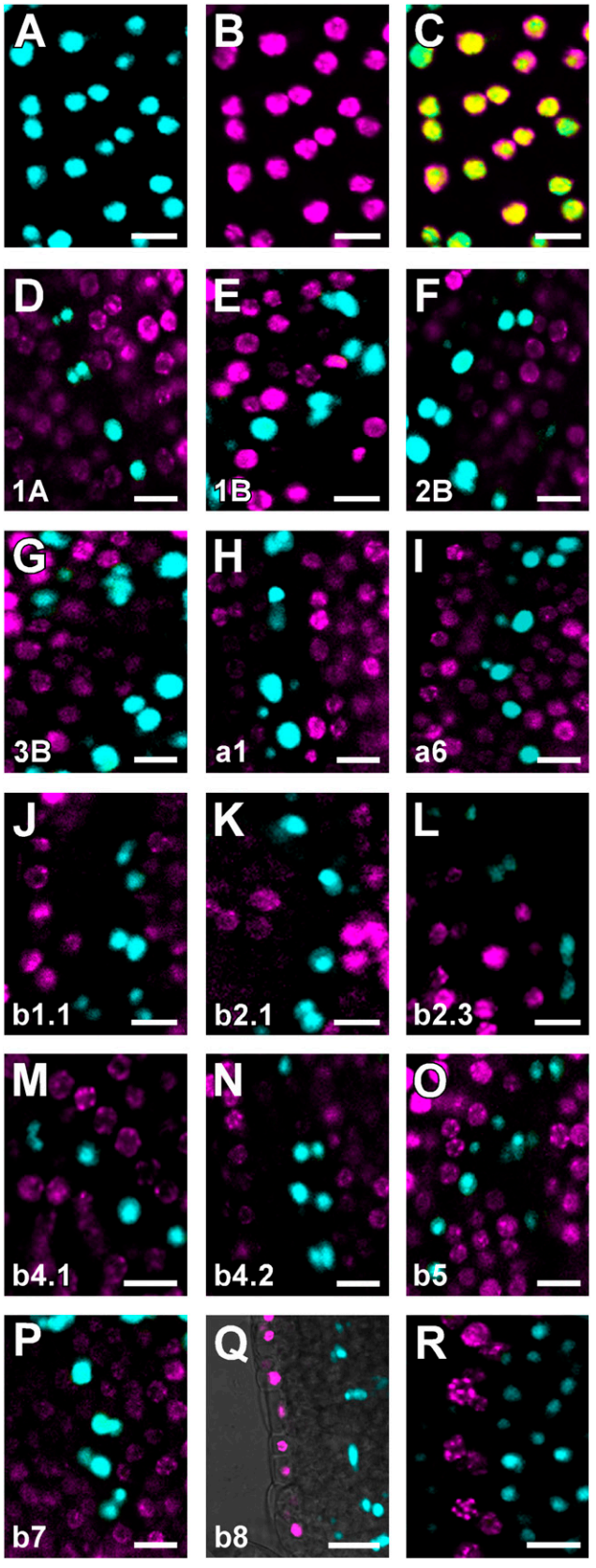

Figure 5. *RbcS* and *Lhc* expression in leaf subepidermal cells. In-figure information and abbreviations are as described in Figure 1. A to P and R, Confocal laser scanning microscopy images of first leaves 4 DAG; leaf tips toward top. Q, Overlay of confocal laser scanning microscopy and transmitted light images. A, $RbcS2B_{pro}$:ECFP:3xNLS expression. B, $RbcS2B_{pro}$:HTA6:EYFP expression. C, Overlay of images in A and B. C to R, Images color-coded with a dual-channel LUT from cyan to magenta through green, yellow, and red (Demandolx and Davoust, 1997). Fluorescence in each detection channel was displayed in either cyan or magenta. Single-fluorophore images were then merged using a differential operator. As a result, preponderance of cyan signal over colocalized magenta signal is encoded in green, opposite in red, and colocalized cyan and magenta signals of equal intensity in yellow. For additional details, see text. D to Q, Cyan, $Athb8_{pro}$:ECFP:3xNLS; magenta, $RbcS_{pro}$:HTA6:EYFP or Lhc_{pro}:HTA6:EYFP as indicated by gene identifier at bottom left. R, Cyan, $RbcS2B_{pro}$:ECFP:3xNLS; magenta, $Athb8_{pro}$:HTA6:EYFP. Bars = 10 μm.

posttranscriptional level (Tobin and Silverthorne, 1985; Simpson and Herrera-Estrella, 1990; Thompson and White, 1991). However, our results are in good agreement with Arabidopsis *RbcS* and *Lhc* expression profiles reported previously (Dedonder et al., 1993; Klimmek et al., 2006) or extracted from publicly accessible large-scale microarray data sets (Birnbaum et al., 2003; Leonhardt et al., 2004; Schmid et al., 2005; Suh et al., 2005; Winter et al., 2007; Supplemental Table S3; Supplemental Fig. S9; and below), suggesting that, at least in Arabidopsis, cellular dynamics of *RbcS* and *Lhc* expression are largely determined by transcription patterns. On the other hand, growth conditions, developmental stages, and spatial resolution in available microarray experiments were often very different from those in our study. Therefore, similarity in expression data should still be interpreted with caution. Because *RbcS* and *Lhc* expression is additionally subject to extensive translational and posttranslational regulation (Tobin and Silverthorne, 1985; Thompson and White, 1991), patterns of gene transcript abundance alone may not necessarily reflect levels of active RbcS and Lhc proteins. However, to our knowledge, none of the reported translational or posttranslational control mechanisms has been shown to impinge on spatiotemporal profiles of *RbcS* and *Lhc* expression, suggesting that cellular patterns of their expression in Arabidopsis development may be accurately visualized by transcriptional fusions. While no expression profiling, at any level or type of resolution, can ever provide direct evidence of gene function, our topography of *RbcS* and *Lhc* expression nonetheless allows us to infer some of their less prominent biological properties.

Uniqueness and Redundancy among *RbcS* and *Lhc* Expression Patterns: Structural and Functional Implications

A major discovery of the Arabidopsis genome sequencing project was the finding that a surprisingly large number of genes encode isoforms of the same polypeptide (The Arabidopsis Genome Initiative, 2000). Large-scale genome duplication events are a common

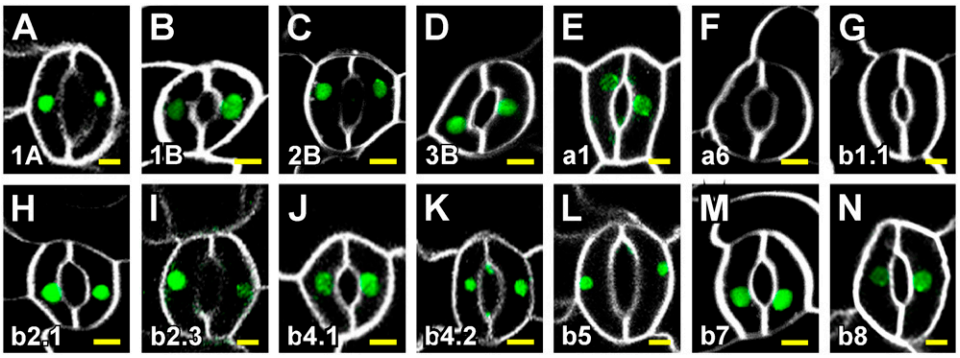

Figure 6. *RbcS* and *Lhc* expression in cotyledon epidermal cells. In-figure information and abbreviations are as described in Figure 1. Confocal laser scanning microscopy images of adaxial epidermis of cotyledons at 4 DAG. Green, $RbcS_{pro}$:HTA6:EYFP or Lhc_{pro}:HTA6:EYFP expression as indicated by gene identifier at bottom left; white, FM 4-64-decorated plasma membrane. Bars = 5 μm.

feature of plant genomes and are mainly responsible for the large number of duplicated individual loci (Bowers et al., 2003; Langham et al., 2004; Paterson et al., 2004; Maere et al., 2005). Duplicate genes may acquire advantageous mutations that become subject to selection and lead to a new function; alternatively, both the ancestral and duplicated gene can accumulate mutations that may lead to the subdivision of the functions of the ancestral gene. These processes of neo- and subfunctionalization occur mainly through mutations in regulatory sequences, rather than mutations in the coding sequence (Blanc and Wolfe, 2004; Haberer et al., 2004; Langham et al., 2004; Wang et al., 2004; Casneuf et al., 2006). If each individual member of a given gene family supplies a set of nonredundant functions, as genetic evidence (Briggs et al., 2006) and evolutionary considerations (Nowak et al., 1997) seem to suggest, diversified expression of gene family members would then provide metabolic diversity and flexibility to individual cells. The physiological fine-tuning of the cell would be further enhanced if protein family members cooperated in multimeric complexes of variable composition. RbcS and Lhc proteins can interact with members of the same family to form heterodimers, trimers, and higher-order complexes (Baker et al., 1975; Jansson, 1994; Ben-Shem et al., 2003; Lucinski et al., 2006). However, the existence of overlapping expression among members of these gene families is a prerequisite for such type of interaction to occur in vivo. Our findings show that, in Arabidopsis, members of the *RbcS* and *Lhc* families are expressed in distinct, yet redundant, spatio-temporal domains, suggesting that the light-harvesting and photosynthetic apparatus may have a different polypeptide composition in different cells and that such composition could change over time even within the same cell. Aggregation status of Lhca6, Lhcb7, and Lhcb8 within the LHCs is yet to be determined, but our results suggest that samples other than mature leaves, the materials typically used in biochemical studies of photosystems, will have to be used to address such a question. In fact, *Lhca6* is expressed only transiently in leaf development and displays inconspicuous, erratic expression in mature leaves, while expression of *Lhcb7* and *Lhcb8* is restricted to a small subpopulation of cells throughout leaf development.

The precise biological function of each member of the *RbcS* and *Lhc* families will eventually have to be defined by single or higher-order loss-of-function mutations, but our results can already serve as a baseline to explore the biological consequences of mutations in these genes. *RbcS1A*, but none of the other *RbcS* genes, is expressed in root tips. Because the *RbcL* gene, which encodes the large, catalytic subunit of Rubisco, is also expressed in root tips (Isono et al., 1997), a functional isoform of the multimeric enzyme may be present in these tissues. Two additional observations in our study support that root tip expression of *RbcS1A* (and *RbcL*) do not represent spurious gene activities, but may be related to yet-to-be-uncovered functions for photosynthetic genes in the root. First, two members of the *Lhc* family, *Lhcb1.1* and *Lhcb4.1*, are also expressed in the root tip. Second, not only are *Lhcb1.1* and *Lhcb4.1* expressed in these tissues, but their cumulative root tip expression domain surprisingly matches that of *RbcS1A*. Global gene expression profiling revealed low levels of expression of *Lhcb4.1* in the root tip (Birnbaum et al., 2003; Supplemental Table S3). Presence of *RbcS* and *Lhcb1* transcripts was also detected (Supplemental Table S3), but their identity could not unambiguously be ascertained because, in the ATH1 GeneChip, the same Affymetrix locus identifier is assigned to all the *RbcS* genes on the one hand and to *Lhcb1.1*, *Lhcb1.2*, and *Lhcb1.3*, collectively, on the other. Finally, more recent proteomics efforts have identified RbcL, RbcS1A, and Lhcb4.1 polypeptides in the Arabidopsis root (Baerenfaller et al., 2008), suggesting that in Arabidopsis *Rbc* and *Lhc* gene expression data largely mirror protein accumulation profiles. Because RbcS and Lhc activity is subject to extensive control at the posttranslational level (Tobin and Silverthorne, 1985; Thompson and White, 1991), even patterns of protein abundance alone may, however,

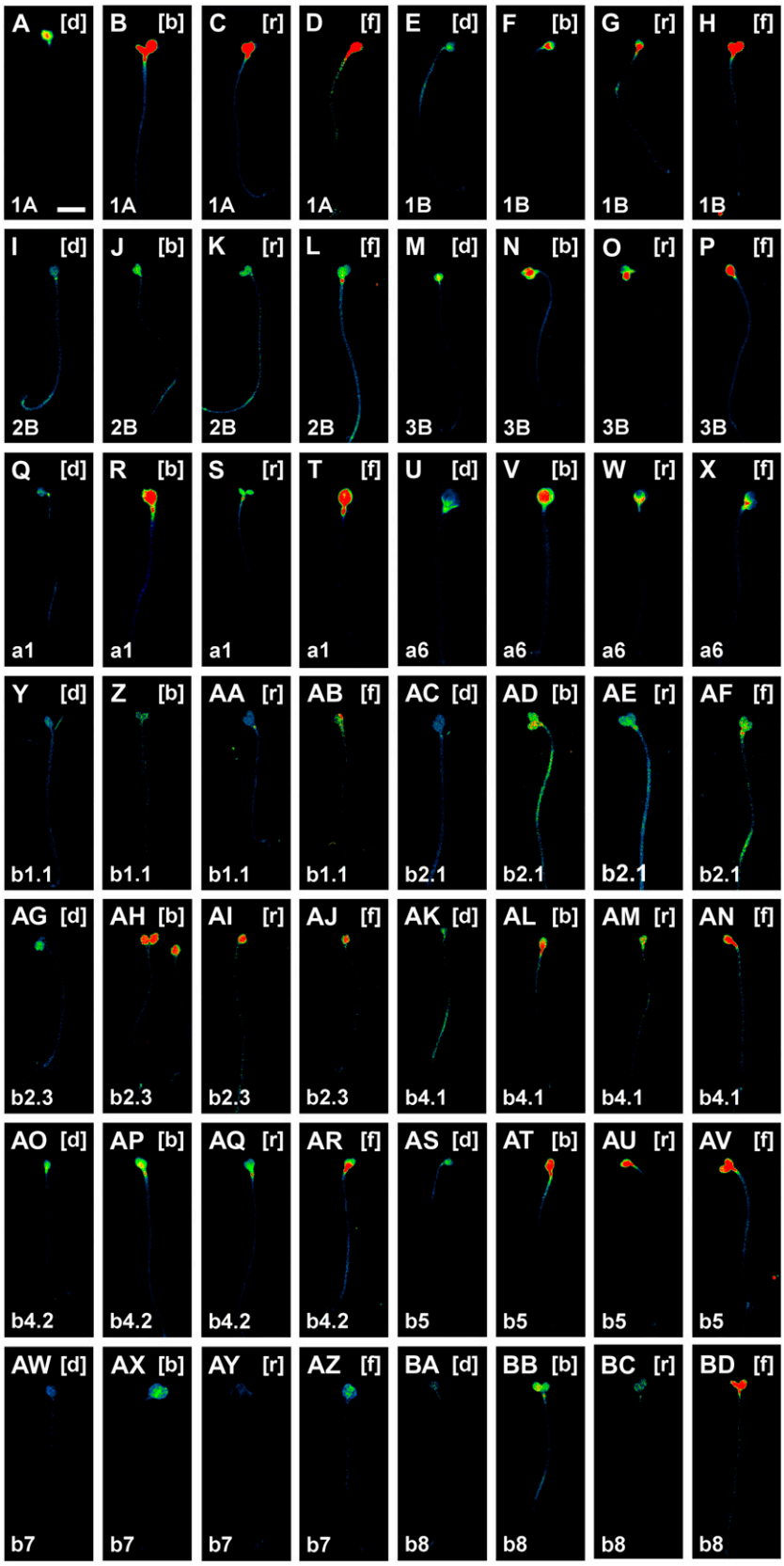

Figure 7. Response of *RbcS* and *Lhc* expression to different light conditions. In-figure information, color code, and abbreviations are as described in Figure 1. Top right, Light treatment. Seedlings are displayed at identical magnification; therefore, for simplicity, scale bars are only reported in the first image. Wide-field epifluorescence microscopy throughout. [b], Seedlings grown for 1 d in blue light following 3 d of growth in the dark; [d], seedlings grown for 4 d in the dark; [f], seedlings grown for 1 d in far-red light following 3 d of growth in the dark; [r], seedlings grown for 1 d in red light following 3 d of growth in the dark. For additional details, see text. Bar = 2 mm.

not necessarily reflect levels of functional RbcS and Lhc proteins. While the significance of the expression of photosynthesis-related genes and proteins in what are generally perceived as photosyntetically inactive tissues still eludes us, our findings suggest a means to uncover the unique biological roles of *RbcS1A*, *Lhcb1.1*, and *Lhcb4.1*. Extensive overlap of gene expression in most plant tissues may preclude dissecting the function of these genes in single mutants, but focusing phenotypic analysis on the root tip could provide the possibility to unequivocally assign a nonredundant function.

Uniqueness and Redundancy among *RbcS* and *Lhc* Expression Patterns: Gene Expression and Developmental Ramifications

Transcriptomes from different plants or organs at different physiological states have generated a vast amount of information that can be monitored and compared. However, data from gene expression profiling of whole plants or entire organs have to be interpreted with caution, as genes that appear to be sporadically expressed at the organ level may be expressed at high levels in very small cellular fields (Kehr, 2003; Brandt, 2005; Lange, 2005; Lee et al., 2005). Furthermore, if only mature stages of organ development are sampled for transcript analysis, ephemeral gene expression may be underestimated or entirely missed. Previous studies identified *Lhca6*, *Lhcb7*, and *Lhcb8* as being rarely expressed in Arabidopsis (Jansson, 1999; Klimmek et al., 2006), a finding that is supported by the extremely low hybridization signal associated with these genes in available microarray data sets (Supplemental Table S3); however, in our study, *Lhca6*, *Lhcb7*, and *Lhcb8* were expressed at levels comparable to those of the abundantly expressed genes *Lhca1* and *Lhcb1.1* (Figs. 1–7; Klimmek et al., 2006). The apparent discrepancy vanishes if one considers that *Lhca6*, *Lhcb7*, and *Lhcb8* are always expressed in a subset of cells in each individual organ. Furthermore, the proportion of cells expressing these genes decreases during organ development, such that at organ maturity, the stage typically sampled in microarray experiments (Supplemental Table S3), expression of *Lhca6*, *Lhcb7*, and *Lhcb8* is maintained in very small cellular domains.

Technologies aimed at characterizing the population of genes that are transcribed in individual cell types, such as fluorescence-activated cell sorting (Birnbaum et al., 2005), are enormously facilitated by, or completely rely on, the availability of cell type-specific markers. Gene expression profiles selectively labeling distinct cell types are already available and have been indispensable to the identification of the gene expression complement of a variety of cells and tissues through single cell-type sampling (Birnbaum et al., 2003; Nawy et al., 2005). However, lack of markers for mesophyll has hampered the extension of those approaches to the characterization of the cohort of genes that molecularly define this tissue. Further, cell state-specific markers have been crucial for the characterization of tissue ontogeny, especially of steps preceding acquisition of morphological conspicuity (e.g. Malamy and Benfey, 1997; Scarpella et al., 2004; Gordon et al., 2007). While the physiological and biochemical properties of mesophyll cells have been the focus of investigation for the past 300 years (for review, see Govindjee et al., 2006), details of their development are largely unexplored, especially in C_3 plants such as Arabidopsis (Pyke and Lopez-Juez, 1999). During leaf development, most of the *RbcS* and *Lhc* genes were expressed in essentially overlapping subepidermal nonvascular domains and with amazingly comparable dynamics, which only seemed to differ for the temporal aspects of the initiation and termination of their expression (Fig. 8). We identified a collection of genes whose onset of expression labeled initial steps of subepidermal tissue ontogeny (*RbcS2B*, *Lhca6*, *Lhcb2.1*, *Lhcb4.1*, and *Lhcb5*), a set of genes that became expressed at early stages of mesophyll development (*RbcS1A*, *RbcS3B*, *Lhca1*, *Lhcb1.1*, and *Lhcb4.2*), and a late marker of mesophyll differentiation (*Lhcb2.3*). Subepidermal cells that initiate expression of genes belonging to the two latter groups (*RbcS1A*, *RbcS3B*, *Lhca1*, *Lhcb1.1*, *Lhcb4.2*, and *Lhcb2.3*) can be discriminated because of accumulation of autofluorescent plastids, acquisition of round cell shape, presence of intercellular spaces, or a combination of those features. However, onset of expression of genes of the first cluster (*RbcS2B*, *Lhca6*, *Lhcb2.1*, *Lhcb4.1*, and *Lhcb5*) identifies a distinct cell state within a population of anatomically indistinguishable ground cells. Sustained levels of expression of this set of genes overlap with initiation of expression of *RbcS* and *Lhc* genes marking onset of mesophyll anatomical differentiation (Fig. 8A). Further, cells that express *RbcS* and *Lhc* genes fail to express the preprocambial marker gene *Athb8*, which labels ground cells specified to a vascular fate. Therefore, we conclude that expression of *RbcS* and *Lhc* genes of the first group identifies a "premesophyll" cell state that cannot be distinguished anatomically. Mutual exclusivity of premesophyll and preprocambial states supports the view that mesophyll and vascular cell identity acquisition represent antagonistic pathways in leaf subepidermal tissue ontogeny (Scarpella et al., 2004; Kang et al., 2007; Sawchuk et al., 2008). While no single regulatory element is unique to the upstream noncoding regions of the genes belonging to each of the three groups of mesophyll developmental stage-specific markers, each of these cohorts of genes is characterized by the presence of a distinct array of overrepresented elements in their upstream sequences (Supplemental Table S4). Regulatory regions of premesophyll genes are characterized by overrepresentation of the Tbox required for promoter activity of genes that are exclusively expressed in green organs (Yang et al., 1993; Kwon et al., 1994; Chan et al., 2001). Further, overrepresentation of the I-box, which has been suggested to mediate photosynthetic

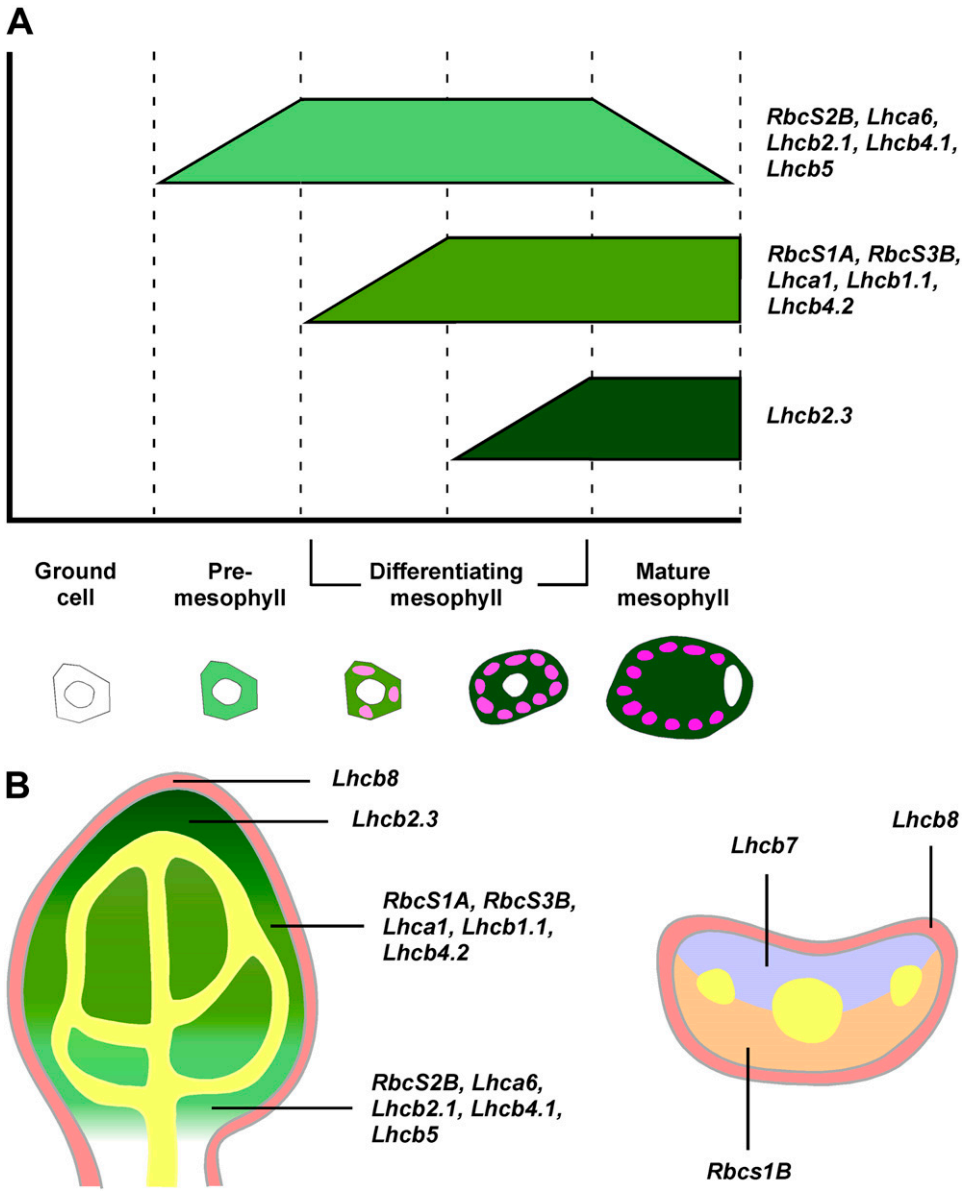

Figure 8. Schematic summary of *RbcS* and *Lhc* expression in leaf development. A, Graphic representation of temporal expression profiles and associated stages of leaf mesophyll cell development. Green bars indicate the duration of maximum expression of each cohort of genes; ramped termini denote gradual initiation or decline of gene expression. B, Tissue map of a paradermal (left) or a transverse (right) median section through a developing leaf illustrating fields of gene expression. Different shades of green indicate consecutive onset of gene expression and corresponding stages of mesophyll ontogeny as defined in A. Orange, abaxial side; pink, epidermis; purple, adaxial side; yellow, preprocambial and procambial cells as visualized through *Athb8* expression (Baima et al., 1995; Kang and Dengler, 2004; Scarpella et al., 2004).

tissue-specific expression (Martinez-Hernandez et al., 2002; Maclean et al., 2008), is unique to upstream sequences of genes labeling intermediate stages of leaf mesophyll development. Finally, the *Lhcb2.3* upstream noncoding region is distinguished by overrepresentation of the Box II necessary for mesophyll-specific expression (Nishiuchi et al., 1995). Although each of these regulatory elements has been implicated in expression in green tissues, their impact on stage-specific expression in leaf mesophyll ontogeny remains to be addressed experimentally.

In our study, adaxial expression of *Lhcb7* and abaxial expression of *RbcS1B* label cells in the leaf that will give rise to palisade and spongy mesophyll, respectively, before any overt anatomical differentiation has taken place (Pyke et al., 1991). Because the adaxial side of the leaf is that which is exposed to the highest light intensity, it is not immediate to reconcile the expression pattern of *Lhcb7* in the leaf with the protein's predicted light-harvesting function in light-limiting conditions. Alternatively, *Lhcb7* could function in nonphotochemical quenching to dissipate energy under conditions where the absorbed light exceeds the electron transfer capacities of the thylakoid complexes contributing to primary photochemistry (Szabo et al., 2005), and a similar function has indeed already been suggested for *Lhcb4*, *Lhcb5*, and *Lhcb6* (Farber et al., 1997; Dall'Osto et al., 2005). Carbon dioxide fixation is proportional to light intensity, but Rubisco content and carbon fixation at the abaxial and adaxial surfaces of the leaf are comparable (Nishio et al., 1993; Sun and Nishio, 2001). This suggests the presence of Rubisco isoforms at the abaxial side that are more efficient in carbon fixation at light-limiting conditions than the

isoforms existing at the adaxial side. *RbcS1B* is the only *RbcS* gene to be exclusively expressed at the abaxial side of the leaf, which suggests that RbcS1B could modify the catalytic properties of Rubisco and increases its enzymatic efficiency in light-limiting conditions. Alternatively, because cells of the spongy mesophyll are separated by extensive intercellular spaces, comparable levels of Rubisco at the abaxial and adaxial surfaces could reflect a higher content of Rubisco per cell in the spongy mesophyll. Because the amount of small Rubisco subunits regulates large subunit expression (Khrebtukova and Spreitzer, 1996; Rodermel et al., 1996), additional RbcS1B at the abaxial side of the leaf could simply be part of a mechanism for regulating Rubisco abundance. The precise assignment of a function to *RbcS1B*, and to *RbcS* genes in general, will, however, have to await the development of methods to quantify the presence or proportion of different small Rubisco subunits in the holoenzyme. Irrespective of the specific role of *RbcS1B*, its upstream noncoding region, but not that of any of the other genes in our study, contains the AACGGGTGAA sequence required for suppression of expression in the adaxial domain of the leaf primordium (Supplemental Table S4; Watanabe and Okada, 2003).

Except for *RbcS2B* and *Lhca6*, whose expression across the entire plant is predominantly or exclusively associated with subepidermal, photosynthetic cells, each of the other genes has additional, conspicuous expression domains in nonmesophyll cells in organs other than the leaf. While it will be interesting to understand the molecular basis of the nonmesophyll expression domains, all the markers can already begin to assist in the spatial and temporal dissection of leaf mesophyll ontogeny, and expression of *RbcS2B* and *Lhca6* can be used to readily visualize and molecularly characterize mesophyll cells and their development throughout the plant.

MATERIALS AND METHODS

Vector Construction

The origins of the $Athb8_{pro}$:ECFP:3xNLS and the $Athb8_{pro}$:HTA6:EYFP lines have been previously described (Sawchuk et al., 2007). To generate the $RbcS_{pro}$:HTA6:EYFP and Lhc_{pro}:HTA6:EYFP lines, sequences upstream of *RbcS* or *Lhc* coding regions, respectively, were amplified from Arabidopsis (*Arabidopsis thaliana*) ecotype Columbia (Col-0) genomic DNA using Finnzymes Phusion high-fidelity DNA polymerase (New England BioLabs) and gene-specific primers (Supplemental Table S1), integrated into pDONR221(Invitrogen) with BP clonase II (Invitrogen), sequence-checked, and recombined into the Gateway-adapted pFYTAG binary vector (Zhang et al., 2005) using LR clonase II (Invitrogen). The $RbcS2B_{pro}$:ECFP:3xNLS line was generated by recombining the pDONR221-integrated *RbcS2B* upstream sequences into the Gateway-adapted pBGCN binary vector (Kubo et al., 2005) with LR clonase II (Invitrogen). To generate the $UBQ10_{pro}$:EGFP:LTi6b line, the EGFP:LTi6b sequence was amplified from genomic DNA of a $Ubi3_{pro}$:EGFP:LTi6b line (Vidaurre et al., 2007; a generous gift of M. Aida and B. Scheres) with the EYFP *Kpn*I Forw (TATGGTACCATGGTGAGCAAGGGCGAG) and pEGAD *Sac*I Rev (CCCGAGCTCAATAAATTCCTCACATAAACCAACG) primers using Finnzymes Phusion high-fidelity DNA polymerase (New England BioLabs), subcloned, sequence-checked, and cloned into a derivative of the pC1300-PolyA binary vector (a kind gift of J. Mathur) to give rise to pC1300-EGFP:LTi6b. Approximately 1.5 kb of sequences upstream of the UBQ10 (At4g05320) coding sequence were amplified from Arabidopsis (ecotype Col-0) genomic DNA with the UBQ10 *Hin*dIII Forw (CTCAAGCTTTCCCATGTTTCTCGTCTGTC) and the UBQ10 *Sma*I Rev (CGACCCGGGCTGTTAATCAGAAAAACTCAG) primers using Finnzymes Phusion high-fidelity DNA polymerase (New England BioLabs), subcloned, sequence-checked, and cloned into pC1300-EGFP:LTi6b to give rise to $UBQ10_{pro}$:EGFP:LTi6b.

Plant Material, Transformation, and Growth Conditions

In all experiments, seeds were surface sterilized, synchronized, and germinated on growth medium (half-strength Murashige and Skoog salts [Sigma-Aldrich], 15 g L^{-1} Suc [Fisher Scientific], 0.5 g L^{-1} MES [Sigma Chemical], 0.8% [w/v] agar [Bioshop Canada], pH 5.7) at a density of 1 seed cm^{-2} as previously described (Scarpella et al., 2004). Sealed plates were incubated at 25°C under continuous fluorescent light ($blue_{450}$:red_{633}:$far\text{-}red_{740}$ 12:22:3 μmol m^{-2} s^{-1}). We define DAG as days following exposure of imbibed seeds to light. For analysis of gene expression under controlled light conditions, germination was induced by incubating sealed plates at 25°C under fluorescent light ($blue_{450}$:red_{633}:$far\text{-}red_{740}$ 12:22:3 μmol m^{-2} s^{-1}) for 2 h. Plates were then wrapped in aluminum foil and incubated at a 70° angle at 25°C in the dark. At 3 DAG, plates were either incubated at 25°C in the dark for an additional 24-h period or unwrapped and incubated at 25°C for 24 h under blue (450 nm: 19 μmol m^{-2} s^{-1}), red (633 nm: 11 μmol m^{-2} s^{-1}), or far-red (740 nm: 7 μmol m^{-2} s^{-1}) light provided by 470-nm, 633-nm, or 731-nm A19 DecorLED 270° solid-state lamps (Ledtronics), respectively. Seedlings were transferred at 5 DAG to Promix BX soil (Evergro/Westgro) in 7- × 7- × 8-cm pots at a density of 0.1 seedlings cm^{-2} and grown at 22°C under fluorescent light ($blue_{450}$:red_{633}:$far\text{-}red_{740}$ 14:88:6 μmol m^{-2} s^{-1}) in a 16-h-light/8-h-dark cycle. Arabidopsis (ecotype Col-0) was transformed with *Agrobacterium tumefaciens* strain GV3101::MP90 (Koncz and Schell, 1986) harboring the $RbcS_{pro}$:HTA6:EYFP, Lhc_{pro}:HTA6:EYFP, or $RbcS2B_{pro}$:ECFP:3xNLS constructs by the floral dip method (Clough and Bent, 1998). Primary transformants were selected on growth medium supplemented with 200 μg mL^{-1} carbenicillin (Bioshop Canada), 10 μg mL^{-1} glufosinate ammonium (Crescent Chemical), and 50 μg mL^{-1} nystatin (Bioshop Canada).

Microtechniques and Microscopy

Whole seedlings, dissected seedling organs, embryos, and stem hand-sections were mounted in water with a 0.17-mm coverslip (Fisher Scientific; VWR). Dissected silique and flower samples were imaged in plastic dishes with water-submerged pedicels. Seedlings, flowers, siliques, and embryos were viewed with a 1× Planapochromat (NA, 0.041; WD, 55 mm) objective of a Leica MZ 16FA stereomicroscope (Leica Microsystems) equipped with an HBO103 mercury vapor short-arc lamp (Osram), and images were captured with an Andor iXon^{EM}+ camera (Andor Technology). YFP was visualized using a 500/20 excitation filter and a 535/30 emission filter (Leica Microsystems). Seedling organs and stem sections were viewed with a 5× Fluar (NA, 0.25; WD, 12.5 mm), 10× Planapochromat (NA, 0.45; WD, 2.0 mm), 20× Planapochromat (NA, 0.8; WD, 0.55 mm), or 40× Planapochromat (NA, 0.95; WD, 0.25 mm) objective of an Axio Imager.M1 microscope (Carl Zeiss) equipped with a Hamamatsu ORCA-AG camera (Hamamatsu Photonics). YFP was visualized with a 50%-attenuated HBO103 mercury vapor short-arc lamp (Osram) using a BP 500/20 excitation filter, an FT515 beam splitter, and a BP 535/30 emission filter (Carl Zeiss). Lignin autofluorescence was visualized using a BP 390/22 excitation filter, an FT420 beam splitter, and a BP 460/50 emission filter (Carl Zeiss). Samples were exposed for 0.05 to 1 s during image acquisition, because longer exposure times induce physiological damage, mitotic arrest, and cell death (Dixit and Cyr, 2003). Electron multiplication gain or output amplifier gain values were set to match the incoming signal with the input range of the camera analog-to-digital converter (Nordberg and Sluder, 2007). For visualization of light responsiveness of gene expression, imaging parameters were optimized for dark-grown samples, and all other samples were imaged at identical settings. Because high resolution is required to achieve visible separation of fluorescence signals that are in close proximity but are not spatially overlapping (Smallcombe, 2001), for colocalization analysis, leaves were observed with a 63× Planaprochromat oil (NA, 1.4; WD, 0.19 mm) objective of a Zeiss Axiovert 100M microscope equipped with a Zeiss LSM 510 laser module confocal unit (Carl Zeiss). For visualization of GFP and YFP, or of CFP and YFP, GFP or CFP was excited with the 458-nm line of an argon laser at 55% of output (equivalent to approximately 6 A) and 85%

to 100% transmission and emission detected with a BP480-520 filter, while YFP was excited with the 514-nm line of an argon laser at 1% to 45% transmission and emission detected with a BP565-615 filter. For visualization of plastid autofluorescence, chlorophyll was excited with the 543-nm line of a helium-neon laser at 3% transmission and emission detected with a BP650-710 filter. For plasma membrane stainings, seedlings were incubated in 10 μg mL^{-1} FM 4-64 (Invitrogen) for 2 min immediately prior to imaging with a 63× Planaprochromat oil (NA, 1.4; WD, 0.19 mm) objective of a Zeiss Axiovert 100M LSM 510 laser scanning confocal microscope (Carl Zeiss). For visualization of YFP and FM 4-64, YFP was excited with the 488-nm line of an argon laser at 5% to 30% transmission and emission detected with a BP500-550 filter, while FM 4-64 was excited with the 543-nm line of a helium neon laser at 5% to 10% transmission and emission detected with a BP565-615 filter. Optical slices of identical thickness were used to collect fluorophore emission signals in multiple labeling experiments, and identical settings were adopted to detect chlorophyll autofluorescence in all samples. Sequential excitation and collection of emission from individual fluorophores were performed in high-speed channel switching (multitrack) line scanning mode. Under these conditions, signal bleed-through of the different fluorophores across different photomultiplier channels was never observed. Signal-to-noise ratio was increased during image acquisition by four-frame temporal averaging (Russ, 2002).

Image Analysis and Processing

All images were cropped using Adobe Photoshop 7.0 (Adobe Systems) and turned into 8-bit images using ImageJ (National Institutes of Health, http://rsb.info.nih.gov/ij). Brightness and contrast were not altered for images of gene expression in different light environments. For all other images, brightness and contrast were adjusted through linear stretching of the histogram in ImageJ (National Institutes of Health). Images were color-displayed by applying in ImageJ (National Institutes of Health) a purposely created LUT in which black was used to encode global background, blue to encode local background, and cyan, green, yellow, orange, and red to encode increasing signal intensities (available as downloadable supplemental file). Signal colocalization was visualized with an extended dual-channel LUT from cyan to magenta through green, yellow, and red (Demandolx and Davoust, 1997). Fluorescence in each detection channel was displayed in either cyan or magenta and then merged using the differential operator in Adobe Photoshop 7.0 (Adobe Systems). As a result, a preponderance of cyan signal over colocalized magenta signal is encoded in green, opposite in red, and colocalized cyan and magenta signals of equal intensity in yellow. All images were assembled into figures and labeled in Canvas 8 (ACD Systems International).

Supplemental Data

The following materials are available in the on-line version of this article.

Supplemental Figure S1. *RbcS* and *Lhc* expression in light-grown seedlings.

Supplemental Figure S2. *RbcS* and *Lhc* expression in seedling organs.

Supplemental Figure S3. *RbcS* and *Lhc* expression in mature plant organs and embryos.

Supplemental Figure S4. *RbcS* and *Lhc* expression during leaf development.

Supplemental Figure S5. *RbcS* and *Lhc* expression in leaf subepidermal cells.

Supplemental Figure S6. *RbcS* and *Lhc* expression in cotyledon epidermal cells.

Supplemental Figure S7. Response of *RbcS* and *Lhc* expression to different light conditions.

Supplemental Figure S8. *RbcS1B* expression in 4- and 6-DAG leaves.

Supplemental Figure S9. Genevestigator-generated organ-specific and developmental *RbcS* and *Lhc* expression chart.

Supplemental Table S1. Genes, loci, and primers.

Supplemental Table S2. Reproducibility criteria and indices.

Supplemental Table S3. *RbcS* and *Lhc* expression levels from publicly available microarray data sets.

Supplemental Table S4. Regulatory elements associated with specific *RbcS* and *Lhc* gene expression patterns.

Supplemental File S1. Additional literature cited.

Supplemental File S2. LUT used in this study.

ACKNOWLEDGMENTS

We thank Mitsuhiro Aida, Taku Demura, David Galbraith, Jaideep Mathur, and Ben Scheres for generously providing plasmids and seeds, Mike Deyholos for help with microarray data set analysis, and Thomas Berleth, Luis Herrera-Estrella, and June Simpson for invaluable comments on the manuscript.

Received July 25, 2008; accepted September 24, 2008; published September 26, 2008.

LITERATURE CITED

Ali S, Taylor WC (2001) The 3′ non-coding region of a C4 photosynthesis gene increases transgene expression when combined with heterologous promoters. Plant Mol Biol **46:** 325–333

Altamura MM, Possenti M, Matteucci A, Baima S, Ruberti I, Morelli G (2001) Development of the vascular system in the inflorescence stem of Arabidopsis. New Phytol **151:** 381–389

Arguello-Astorga G, Herrera-Estrella L (1998) Evolution of light-regulated plant promoters. Annu Rev Plant Physiol Plant Mol Biol **49:** 525–555

Baerenfaller K, Grossmann J, Grobei MA, Hull R, Hirsch-Hoffmann M, Yalovsky S, Zimmermann P, Grossniklaus U, Gruissem W, Baginsky S (2008) Genome-scale proteomics reveals Arabidopsis thaliana gene models and proteome dynamics. Science **320:** 938–941

Baima S, Nobili F, Sessa G, Lucchetti S, Ruberti I, Morelli G (1995) The expression of the Athb-8 homeobox gene is restricted to provascular cells in Arabidopsis thaliana. Development **121:** 4171–4182

Baker TS, Eisenberg D, Eiserling FA, Weissman L (1975) The structure of form I crystals of D-ribulose-1,5-diphosphate carboxylase. J Mol Biol **91:** 391–399

Bansal KC, Viret JF, Haley J, Khan BM, Schantz R, Bogorad L (1992) Transient expression from cab-m1 and rbcS-m3 promoter sequences is different in mesophyll and bundle sheath cells in maize leaves. Proc Natl Acad Sci USA **89:** 3654–3658

Bedbrook JR, Coen DM, Beaton AR, Bogorad L, Rich A (1979) Location of the single gene for the large subunit of ribulosebisphosphate carboxylase on the maize chloroplast chromosome. J Biol Chem **254:** 905–910

Ben-Shem A, Frolow F, Nelson N (2003) Crystal structure of plant photosystem I. Nature **426:** 630–635

Birnbaum K, Jung JW, Wang JY, Lambert GM, Hirst JA, Galbraith DW, Benfey PN (2005) Cell type-specific expression profiling in plants via cell sorting of protoplasts from fluorescent reporter lines. Nat Methods **2:** 615–619

Birnbaum K, Shasha DE, Wang JY, Jung JW, Lambert GM, Galbraith DW, Benfey PN (2003) A gene expression map of the Arabidopsis root. Science **302:** 1956–1960

Blanc G, Wolfe KH (2004) Functional divergence of duplicated genes formed by polyploidy during *Arabidopsis* evolution. Plant Cell **16:** 1679–1691

Bowers JE, Chapman BA, Rong J, Paterson AH (2003) Unravelling angiosperm genome evolution by phylogenetic analysis of chromosomal duplication events. Nature **422:** 433–438

Brandt SP (2005) Microgenomics: gene expression analysis at the tissue-specific and single-cell levels. J Exp Bot **56:** 495–505

Briggs GC, Osmont KS, Shindo C, Sibout R, Hardtke CS (2006) Unequal genetic redundancies in Arabidopsis: a neglected phenomenon? Trends Plant Sci **11:** 492–498

Casneuf T, De Bodt S, Raes J, Maere S, Van de Peer Y (2006) Nonrandom divergence of gene expression following gene and genome duplications in the flowering plant Arabidopsis thaliana. Genome Biol **7:** R13

Chan CS, Guo L, Shih MC (2001) Promoter analysis of the nuclear gene encoding the chloroplast glyceraldehyde-3-phosphate dehydrogenase B subunit of Arabidopsis thaliana. Plant Mol Biol **46:** 131–141

Chen M, Chory J, Fankhauser C (2004) Light signal transduction in higher plants. Annu Rev Genet **38:** 87–117

Clough S, Bent A (1998) Floral dip: a simplified method for transformation of Arabidopsis. Plant J **16:** 735–743

Dall'Osto L, Caffarri S, Bassi R (2005) A mechanism of nonphotochemical energy dissipation, independent from PsbS, revealed by a conformational change in the antenna protein CP26. Plant Cell **17:** 1217–1232

Dean C, Pichersky E, Dunsmuir P (1989) Structure, evolution, and regulation of RbcS genes in higher plants. Annu Rev Plant Physiol Plant Mol Biol **40:** 415–439

Dedonder A, Rethy R, Fredericq H, Van Montagu M, Krebbers E (1993) Arabidopsis rbcS genes are differentially regulated by light. Plant Physiol **101:** 801–808

Demandolx D, Davoust J (1997) Multicolour analysis and local image correlation in confocal microscopy. J Microsc **185:** 21–36

Dixit R, Cyr R (2003) Cell damage and reactive oxygen species production induced by fluorescence microscopy: effect on mitosis and guidelines for non-invasive fluorescence microscopy. Plant J **36:** 280–290

Dobbie IM, Lowndes NF, Sullivan KF (2008) Autofluorescent proteins. *In* KF Sullivan, ed, Fluorescent Proteins, Ed 2, Vol 85. Academic Press, London, pp 1–22

Fankhauser C, Chory J (1997) Light control of plant development. Annu Rev Cell Dev Biol **13:** 203–229

Farber A, Young AJ, Ruban AV, Horton P, Jahns P (1997) Dynamics of xanthophyll-cycle activity in different antenna subcomplexes in the photosynthetic membranes of higher plants (the relationship between zeaxanthin conversion and nonphotochemical fluorescence quenching). Plant Physiol **115:** 1609–1618

Fleming AJ, Manzara T, Gruissem W, Kuhlemeier C (1996) Fluorescent imaging of GUS activity and RT-PCR analysis of gene expression in the shoot apical meristem. Plant J **10:** 745–754

Franklin KA, Larner VS, Whitelam GC (2005) The signal transducing photoreceptors of plants. Int J Dev Biol **49:** 653–664

Gordon SP, Heisler MG, Reddy GV, Ohno C, Das P, Meyerowitz EM (2007) Pattern formation during de novo assembly of the Arabidopsis shoot meristem. Development **134:** 3539–3548

Govindjee, Beatty JT, Gest H, Allen JF, editors (2006) Discoveries in Photosynthesis, Vol 20. Springer, Dordrecht, The Netherlands

Grossman AR, Bhaya D, Apt KE, Kehoe DM (1995) Light-harvesting complexes in oxygenic photosynthesis: diversity, control, and evolution. Annu Rev Genet **29:** 231–288

Haberer G, Hindemitt T, Meyers BC, Mayer KF (2004) Transcriptional similarities, dissimilarities, and conservation of cis-elements in duplicated genes of Arabidopsis. Plant Physiol **136:** 3009–3022

Isono K, Niwa Y, Satoh K, Kobayashi H (1997) Evidence for transcriptional regulation of plastid photosynthesis genes in Arabidopsis thaliana roots. Plant Physiol **114:** 623–630

Jansson S (1994) The light-harvesting chlorophyll a/b-binding proteins. Biochim Biophys Acta **1184:** 1–19

Jansson S (1999) A guide to the Lhc genes and their relatives in Arabidopsis. Trends Plant Sci **4:** 236–240

Jefferson RA, Kavanagh TA, Bevan MW (1987) GUS fusions: beta-glucuronidase as a sensitive and versatile gene fusion marker in higher plants. EMBO J **6:** 3901–3907

Jensen RG, Bahr JT (1977) Ribulose 1,5-bisphosphate carboxylase-oxygenase. Annu Rev Plant Physiol **28:** 379–400

Joly E (2007) Optimising blue fluorescent protein (BFP) for use as a mammalian reporter gene in parallel with Green Fluorescent Protein (GFP). Nature Precedings. http://hdl.handle.net/10101/npre.2007.1259.1 (May 15, 2008)

Kang J, Dengler N (2004) Vein pattern development in adult leaves of Arabidopsis thaliana. Int J Plant Sci **165:** 231–242

Kang J, Mizukami Y, Wang H, Fowke L, Dengler NG (2007) Modification of cell proliferation patterns alters leaf vein architecture in Arabidopsis thaliana. Planta **226:** 1207–1218

Kato N, Pontier D, Lam E (2002) Spectral profiling for the simultaneous observation of four distinct fluorescent proteins and detection of protein-protein interaction via fluorescence resonance energy transfer in tobacco leaf nuclei. Plant Physiol **129:** 931–942

Kehr J (2003) Single cell technology. Curr Opin Plant Biol **6:** 617–621

Khrebtukova I, Spreitzer RJ (1996) Elimination of the Chlamydomonas gene family that encodes the small subunit of ribulose-1,5-bisphosphate carboxylase/oxygenase. Proc Natl Acad Sci USA **93:** 13689–13693

Klimmek F, Sjodin A, Noutsos C, Leister D, Jansson S (2006) Abundantly and rarely expressed Lhc protein genes exhibit distinct regulation patterns in plants. Plant Physiol **140:** 793–804

Koncz C, Schell J (1986) The promoter of the TL-DNA gene 5 controls the tissue specific expression of chimaeric genes carried by a novel type of Agrobacterium binary vector. Mol Gen Genet **204:** 383–396

Krebbers E, Seurinck J, Herdies L, Cashmore AR, Timko MP (1988) 4 Genes in 2 Diverged Subfamilies Encode the Ribulose-1,5-Bisphosphate Carboxylase Small Subunit Polypeptides of Arabidopsis-Thaliana. Plant Mol Biol **11:** 745–759

Kubo M, Udagawa M, Nishikubo N, Horiguchi G, Yamaguchi M, Ito J, Mimura T, Fukuda H, Demura T (2005) Transcription switches for protoxylem and metaxylem vessel formation. Genes Dev **19:** 1855–1860

Kwon HB, Park SC, Peng HP, Goodman HM, Dewdney J, Shih MC (1994) Identification of a light-responsive region of the nuclear gene encoding the B subunit of chloroplast glyceraldehyde 3-phosphate dehydrogenase from Arabidopsis thaliana. Plant Physiol **105:** 357–367

Langdale JA, Rothermel BA, Nelson T (1988) Cellular pattern of photosynthetic gene expression in developing maize leaves. Genes Dev **2:** 106–115

Lange BM (2005) Single-cell genomics. Curr Opin Plant Biol **8:** 236–241

Langham RJ, Walsh J, Dunn M, Ko C, Goff SA, Freeling M (2004) Genomic duplication, fractionation and the origin of regulatory novelty. Genetics **166:** 935–945

Lee JY, Colinas J, Wang JY, Mace D, Ohler U, Benfey PN (2006) Transcriptional and posttranscriptional regulation of transcription factor expression in Arabidopsis roots. Proc Natl Acad Sci USA **103:** 6055–6060

Lee JY, Levesque M, Benfey PN (2005) High-throughput RNA isolation technologies. New tools for high-resolution gene expression profiling in plant systems. Plant Physiol **138:** 585–590

Leonhardt N, Kwak JM, Robert N, Waner D, Leonhardt G, Schroeder JI (2004) Microarray expression analyses of *Arabidopsis* guard cells and isolation of a recessive abscisic acid hypersensitive protein phosphatase 2C mutant. Plant Cell **16:** 596–615

Leutwiler LS, Meyerowitz EM, Tobin EM (1986) Structure and expression of three light-harvesting chlorophyll a/b-binding protein genes in Arabidopsis thaliana. Nucleic Acids Res **14:** 4051–4064

Lucinski R, Schmid VH, Jansson S, Klimmek F (2006) Lhca5 interaction with plant photosystem I. FEBS Lett **580:** 6485–6488

Maclean D, Jerome CA, Brown AP, Gray JC (2008) Co-regulation of nuclear genes encoding plastid ribosomal proteins by light and plastid signals during seedling development in tobacco and Arabidopsis. Plant Mol Biol **66:** 475–490

Maere S, De Bodt S, Raes J, Casneuf T, Van Montagu M, Kuiper M, Van de Peer Y (2005) Modeling gene and genome duplications in eukaryotes. Proc Natl Acad Sci USA **102:** 5454–5459

Malamy JE, Benfey PN (1997) Organization and cell differentiation in lateral roots of Arabidopsis thaliana. Development **124:** 33–44

Martinez-Hernandez A, Lopez-Ochoa L, Arguello-Astorga G, Herrera-Estrella L (2002) Functional properties and regulatory complexity of a minimal RBCS light-responsive unit activated by phytochrome, cryptochrome, and plastid signals. Plant Physiol **128:** 1223–1233

McGrath JM, Terzaghi WB, Sridhar P, Cashmore AR, Pichersky E (1992) Sequence of the fourth and fifth Photosystem II type I chlorophyll a/b-binding protein genes of Arabidopsis thaliana and evidence for the presence of a full complement of the extended CAB gene family. Plant Mol Biol **19:** 725–733

Meier I, Callan KL, Fleming AJ, Gruissem W (1995) Organ-specific differential regulation of a promoter subfamily for the ribulose-1,5-bisphosphate carboxylase/oxygenase small subunit genes in tomato. Plant Physiol **107:** 1105–1118

Nawy T, Lee JY, Colinas J, Wang JY, Thongrod SC, Malamy JE, Birnbaum K, Benfey PN (2005) Transcriptional profile of the *Arabidopsis* root quiescent center. Plant Cell **17:** 1908–1925

Nishio JN, Sun J, Vogelmann TC (1993) Carbon fixation gradients across spinach leaves do not follow internal light gradients. Plant Cell **5:** 953–961

Nishiuchi T, Nakamura T, Abe T, Kodama H, Nishimura M, Iba K (1995) Tissue-specific and light-responsive regulation of the promoter region of the Arabidopsis thaliana chloroplast omega-3 fatty acid desaturase gene (FAD7). Plant Mol Biol **29:** 599–609

Nordberg JJ, Sluder G (2007) Practical aspects of adjusting digital cameras. *In* G Sluder, DE Wolf, eds, Digital Microscopy, Ed 3, Vol 81. Academic Press, San Diego, pp 159–169

Nowak MA, Boerlijst MC, Cooke J, Smith JM (1997) Evolution of genetic redundancy. Nature **388:** 167–171

Paterson AH, Bowers JE, Chapman BA (2004) Ancient polyploidization predating divergence of the cereals, and its consequences for comparative genomics. Proc Natl Acad Sci USA **101:** 9903–9908

Pyke K, Lopez-Juez E (1999) Cellular differentiation and leaf morphogenesis in Arabidopsis. Crit Rev Plant Sci **18:** 527–546

Pyke KA, Marrison JL, Leech RM (1991) Temporal and spatial development of the cells of the expanding 1st leaf of Arabidopsis thaliana (L) Heynh. J Exp Bot **42:** 1407–1416

Pyke KA, Page AM (1998) Plastid ontogeny during petal development in Arabidopsis. Plant Physiol **116:** 797–803

Rodermel S, Haley J, Jiang CZ, Tsai CH, Bogorad L (1996) A mechanism for intergenomic integration: abundance of ribulose bisphosphate carboxylase small-subunit protein influences the translation of the large-subunit mRNA. Proc Natl Acad Sci USA **93:** 3881–3885

Russ JC (2002) The Image Processing Handbook, Ed 4. CRC, Boca Raton, FL

Sawchuk MG, Donner TJ, Scarpella E (2008) Auxin transport-dependent, stage-specific dynamics of leaf vein formation. Plant Signal Behav **3:** 286–289

Sawchuk MG, Head P, Donner TJ, Scarpella E (2007) Time-lapse imaging of Arabidopsis leaf development shows dynamic patterns of procambium formation. New Phytol **176:** 560–571

Scarpella E, Francis P, Berleth T (2004) Stage-specific markers define early steps of procambium development in Arabidopsis leaves and correlate termination of vein formation with mesophyll differentiation. Development **131:** 3445–3455

Schmid M, Davison TS, Henz SR, Pape UJ, Demar M, Vingron M, Scholkopf B, Weigel D, Lohmann JU (2005) A gene expression map of Arabidopsis thaliana development. Nat Genet **37:** 501–506

Silverthorne J, Tobin EM (1990) Post-transcriptional regulation of organ-specific expression of individual rbcS mRNAs in Lemna gibba. Plant Cell **2:** 1181–1190

Simpson J, Herrera-Estrella L (1990) Light-regulated gene expression. Crit Rev Plant Sci **9:** 95–109

Smallcombe A (2001) Multicolor imaging: the important question of co-localization. Biotechniques **30:** 1240–1242, 1244–1246

Smyth DR, Bowman JL, Meyerowitz EM (1990) Early flower development in *Arabidopsis*. Plant Cell **2:** 755–767

Suh MC, Samuels AL, Jetter R, Kunst L, Pollard M, Ohlrogge J, Beisson F (2005) Cuticular lipid composition, surface structure, and gene expression in Arabidopsis stem epidermis. Plant Physiol **139:** 1649–1665

Sun J, Nishio J (2001) Why abaxial illumination limits photosynthetic carbon fixation in spinach leaves. Plant Cell Physiol **42:** 1–8

Szabo I, Bergantino E, Giacometti GM (2005) Light and oxygenic photosynthesis: energy dissipation as a protection mechanism against photooxidation. EMBO Rep **6:** 629–634

Terzaghi WB, Cashmore AR (1995) Light-regulated transcription. Annu Rev Plant Physiol Plant Mol Biol **46:** 445–474

The Arabidopsis Genome Initiative (2000) Analysis of the genome sequence of the flowering plant Arabidopsis thaliana. Nature **408:** 796–815

Thompson WF, White MJ (1991) Physiological and molecular studies of light-regulated nuclear genes in higher plants. Annu Rev Plant Physiol Plant Mol Biol **42:** 423–466

Tobin EM, Silverthorne J (1985) Light regulation of gene expression in higher plants. Annu Rev Plant Physiol **36:** 569–593

Vidaurre DP, Ploense S, Krogan NT, Berleth T (2007) AMP1 and MP antagonistically regulate embryo and meristem development in Arabidopsis. Development **134:** 2561–2567

Wang J, Tian L, Madlung A, Lee HS, Chen M, Lee JJ, Watson B, Kagochi T, Comai L, Chen ZJ (2004) Stochastic and epigenetic changes of gene expression in Arabidopsis polyploids. Genetics **167:** 1961–1973

Watanabe K, Okada K (2003) Two discrete cis elements control the Abaxial side-specific expression of the FILAMENTOUS FLOWER gene in *Arabidopsis*. Plant Cell **15:** 2592–2602

Winter D, Vinegar B, Nahal H, Ammar R, Wilson GV, Provart NJ (2007) An "electronic fluorescent pictograph" browser for exploring and analyzing large-scale biological data sets. PLoS ONE **2:** e718

Yang Y, Kwon HB, Peng HP, Shih MC (1993) Stress responses and metabolic regulation of glyceraldehyde-3-phosphate dehydrogenase genes in Arabidopsis. Plant Physiol **101:** 209–216

Zhang C, Gong FC, Lambert GM, Galbraith DW (2005) Cell type-specific characterization of nuclear DNA contents within complex tissues and organs. Plant Methods **1:** 7